

Unifying Robot Optimization: Monte Carlo Tree Search with Tensor Factorization

Teng Xue^{1,2*}, Amirreza Razmjoo^{1,2†}, Yan Zhang^{1,2†}, Sylvain Calinon^{1,2}

¹Idiap Research Institute, Martigny, Switzerland

²École Polytechnique Fédérale de Lausanne (EPFL), Lausanne, Switzerland

*Corresponding author. Email: teng.xue@idiap.ch

†These authors contributed equally to this work. The authors' names are listed in alphabetical order.

Many robotic tasks, such as inverse kinematics, motion planning, and optimal control, can be formulated as optimization problems. Solving these problems involves addressing nonlinear kinematics, complex contact dynamics, and long-horizon planning, each posing distinct challenges for state-of-the-art optimization methods. To efficiently solve a wide range of tasks across varying scenarios, researchers either develop specialized algorithms for the task to achieve, or switch between different frameworks. Monte Carlo Tree Search (MCTS) is a general-purpose decision-making tool that enables strategic exploration across problem instances without relying on task-specific structures. However, MCTS suffers from combinatorial complexity, leading to slow convergence and high memory usage. To address this limitation, we propose *Tensor Train Tree Search* (TTTS), which leverages tensor factorization to exploit the separable structure of decision trees. This yields a low-rank, linear-complexity representation that significantly reduces both computation time and storage requirements. We prove that TTTS can efficiently reach the bounded global optimum within a finite time. Experimental results across inverse kinematics, motion planning around obstacles, multi-stage motion

planning, and bimanual whole-body manipulation demonstrate the efficiency of TTTS on a diverse set of robotic tasks.

Introduction

Optimization plays a critical role in robotics and serves as the foundation for a wide range of tasks, including inverse kinematics (1), obstacle avoidance (2), multi-stage motion planning (3), and contact-rich manipulation (4, 5), see Fig. 1. Solving these problems requires addressing inherent nonlinear robot kinematics, non-convex constraints, joint reasoning over discrete contact modes and continuous motion trajectories, as well as complex interactions with the environment—each of which presents substantial challenges for state-of-the-art optimization methods. Specifically, the nonlinearity intrinsic to robotics renders many of these problems non-convex, making gradient-based methods prone to getting trapped in poor local optima (6, 7). Similarly, the need to jointly optimize over discrete modes and continuous motion introduces significant combinatorial complexity, substantially increasing computational costs and slowing convergence for both sampling-based (8, 9) and search-based (10) approaches. To cope with these challenges, general formulations are often discarded to instead focus on specific problems to solve by exploiting the problem structures. For example, trajectory optimization is often addressed through convex optimization with local linearization (11, 12). Obstacle avoidance is typically tackled using sampling-based methods, assuming that the environment contains a sufficiently large free space (13). Contact-rich manipulation—a significantly more challenging task involving hybrid dynamics—is often tackled through local smoothing (14) or the use of complementarity constraints (15, 16). Different optimization techniques can also be combined hierarchically to solve more complex tasks such as aggressive quadrotor flight (17), global optimization around obstacles (2), and fast continuous-time motion planning (18).

While these approaches are effective for specific tasks, they lack generalizability across domains, limiting their applicability for multi-task autonomy. More importantly, some problems, such as multi-stage motion planning (3, 19) (aka. task and motion planning (20)), are inherently coupled and cannot be decomposed into independent subproblems that can be solved separately. In such cases, discrete mode sequencing and continuous trajectory optimization must be considered jointly.

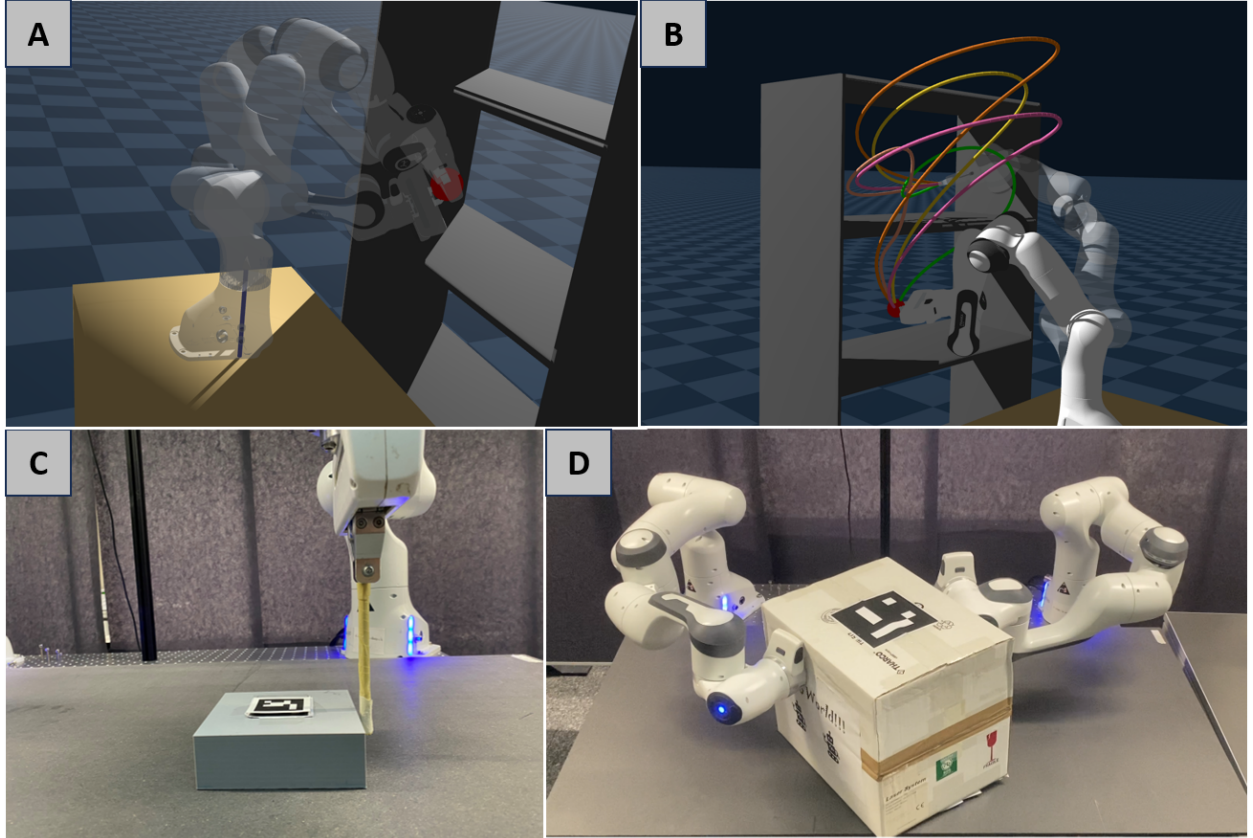


Figure 1: Overview of diverse applicable domains. We demonstrate that TTTS is widely applicable in many tasks, such as Inverse Kinematics (A), Motion Planning (B), Multi-stage Motion Planning (C) and Bimanual Whole-body Manipulation (D).

These challenges highlight the need of a general formulation for robot decision-making. Decision tree (21) offers a compelling representation: it eliminates reliance on gradient information, thereby avoiding poor local optima and making it well-suited for handling nonconvex constraints, nonlinear kinematics and dynamics. Furthermore, the continuous domain can be discretized into tree nodes, enabling joint modeling of both discrete and continuous decision variables. Among decision-making algorithms that utilize such structures, Monte Carlo Tree Search (MCTS) stands out for its strategic exploration capabilities and theoretical guarantee of asymptotic global convergence.

While MCTS offers a general formulation for non-convex and hybrid optimization, it suffers from the curse of dimensionality. To address this issue, Rivère *et al.* proposed to decompose continuous dynamical systems using the spectrum of locally linearized controllability Gramian, which reduces tree size significantly (22). However, this technique is limited to problems with continuous state-action spaces and does not extend well to hybrid discrete-continuous decision-making, as required in multi-stage problems. Additionally, the use of local linearization in high-dimensional, nonlinear systems such as robotic manipulators can still lead to an explosion in tree size. An alternative approach is to approximate the decision tree using neural networks (NNs) (23), which can learn heuristics to accelerate the search process and compress tree information. However, heuristic learning often requires extensive domain knowledge or exhaustive training data and tends to generalize poorly to new problem settings. For instance, while AlphaGo (24) demonstrated superhuman performance in Go using learned heuristics, those models cannot be easily transferred to different domains. Furthermore, although NNs can reduce storage costs, their approximations are typically local (limited to visited nodes), which restricts the accuracy of the learned heuristics and their effectiveness in guiding global search.

In this article, we address the curse of dimensionality in decision trees by modeling a multi-layer tree as a high-dimensional tensor and applying tensor factorization to exploit its inherent structure. Specifically, we introduce *Tensor Train Tree Search* (TTTS), which encodes the tree in *Tensor Train* (TT) format—a compact representation that expresses high-dimensional tensors as sequences of third-order cores with significantly fewer elements, each associated with a specific dimension (i.e., a tree layer). Unlike the widely used node- and table-based representations, TT enables full parallelization of MCTS, significantly reducing search time with linear scaling. The

separable structure of TT further transforms the original tree—characterized by combinatorial complexity—into a form with linear complexity in both time and space perspective, resulting in exponential reductions in computation and memory requirements.

The TT representation serves as a low-rank approximation of the underlying decision tree and acts as a global heuristic to guide the selection and simulation process. By combining TT approximation with MCTS-based search, our algorithm efficiently converges to a bounded global optimum (within a parameterized class of trajectories) in finite time.

Our main contributions are as follows:

1. We propose a general formulation for decision making in robotics that can handle nonlinear dynamical systems, non-convex constraints, hybrid state-action spaces, and multi-modal solution discovery.
2. We introduce the use of Tensor Train (TT) as a novel representation of decision trees, where its separable structure enables fully parallel tree search and achieves linear time and space complexity for efficient decision-making.
3. We provide theoretical guarantees, proving bounded and fast global convergence for general decision making.
4. We evaluate our approach against state-of-the-art methods and demonstrate its effectiveness on inverse kinematics, motion planning around obstacles, multi-stage motion planning, and real-world bimanual whole-body manipulation tasks.

Results

We first applied our approach to simple continuous optimization and mixed-integer programming problems to motivate our work and provide intuition for the reader. We then demonstrate the effectiveness of the proposed mathematical formulation and solver on a diverse set of robotic tasks, including inverse kinematics, motion planning around obstacles, multi-stage motion planning, and bimanual whole-body manipulation. The breadth of these experiments highlights the general applicability of TTTS, with a wide range of robot optimization problems. We also conduct ablation

studies to evaluate the contribution of each component, along with numerical comparisons against state-of-the-art baselines to assess overall performance.

Toy examples

Continuous optimization

We begin by optimizing a non-convex continuous function to build intuition. As shown in Fig. 2a, the function exhibits multiple local optima, highlighting strong multimodality. Such multimodality often causes gradient-based methods and single-modal evolutionary algorithms (e.g., CMA-ES) to become trapped in local optima. In contrast, the Tensor Train (TT) approach reformulates the optimization problem as density estimation, enabling it to capture multimodal structures. The resulting factorized representation reveals a separable structure across dimensions, which facilitates the fast discovery of globally optimal solutions. However, existing TT-based optimization methods such as those in (25, 26), typically require the function to be low-rank—an assumption that might not hold in many practical scenarios. For instance, the function in Fig. 2a can be interpreted as a cost function in an obstacle avoidance task. Its discrete matrix analogue, shown in Fig. 2b, clearly demonstrates full-rank characteristics. To illustrate both the strengths and limitations of low-rank approximation (i.e., approximating a high-rank function using a tensor with lower ranks), we set the TT rank to $r_{max} = 2$ and construct TT approximation using TT-Cross (27, 28), which is an efficient algorithm for computing TT decomposition without requiring access to all entries of the original tensor. It selects informative submatrices via the maximum volume principle to build a global approximation from limited samples, enabling scalable modeling of high-dimensional functions.

The results are depicted in Fig. 2c, which shows that, despite using a much lower rank, TT-Cross effectively captures the structure of the function and enables rapid localization of regions likely to contain optimal solutions. However, TT-Cross relies on cross approximation through submatrices, but selecting these submatrices is an NP-hard problem. And the original function may have a significantly higher rank than the maximum TT-rank permitted by storage constraints, which limits the accuracy of TT approximation. Due to these factors, TT-Cross alone can sometimes yield imprecise function approximations, adversely impacting the solution-finding process. TTGO (25) relies on TT-Cross to obtain the TT model, where the quality of the optimization solution depends

heavily on the accuracy of this approximation. This limitation motivates the proposed TTTS method, which combines the strengths of the TT approximation (serving as a heuristic that can be quickly obtained for any decision tree) with the strategic search capabilities of MCTS. This synergy enables TTTS to efficiently converge to the global optimum, as illustrated in Fig. 2a.

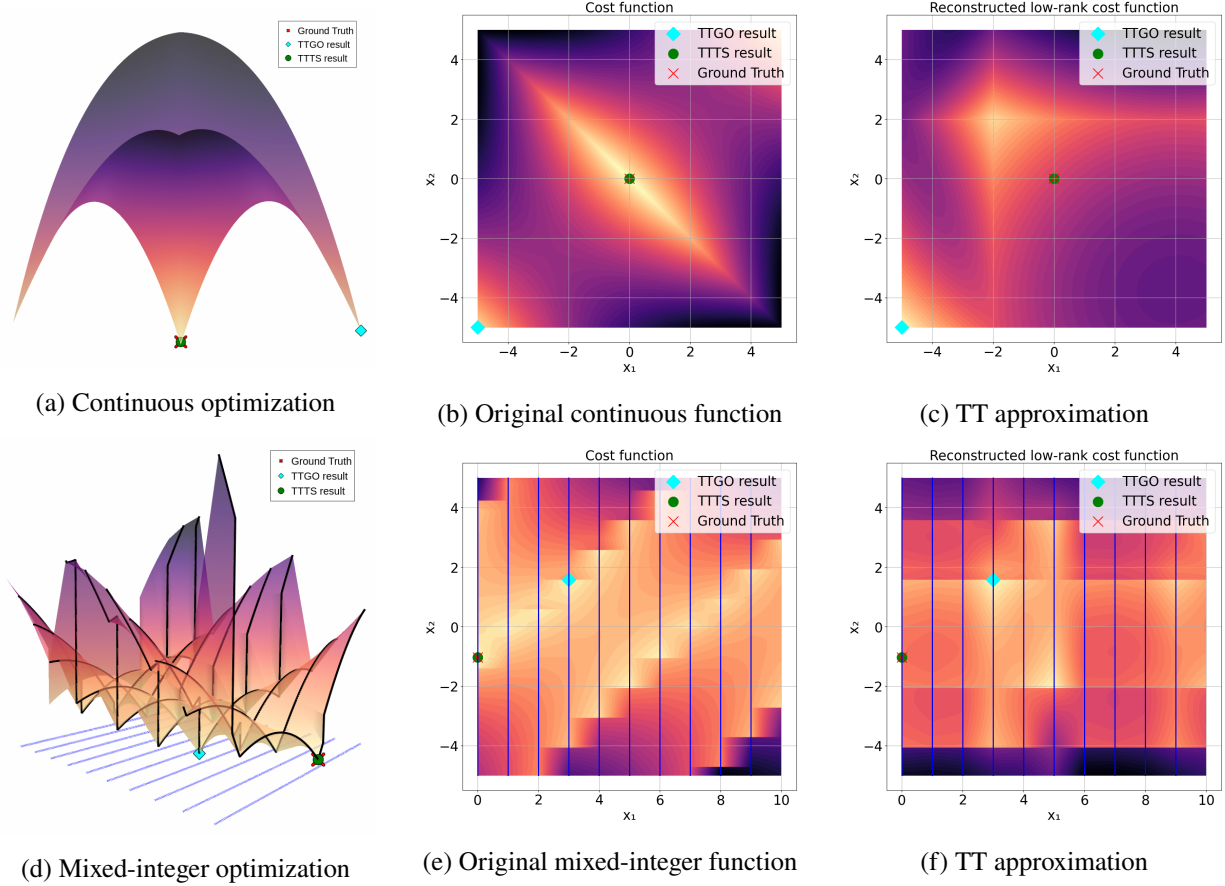


Figure 2: Function optimization and low-rank TT approximation.

Mixed-integer programming

We further demonstrate the effectiveness of our approach in tackling a more challenging problem: mixed-integer nonlinear programming (MINLP). Such problems include both non-convexity due to nonlinear constraints and the combinatorial complexity imposed by integer variables. This setting is particularly difficult because integer variables are discrete and lack gradient information, rendering standard nonlinear programming (NLP) solvers ineffective. An alternative is to discretize the continuous variables and solve the problem using discrete search methods (e.g., A^* or MCTS),

but these approaches typically suffers from the curse of dimensionality and are computationally inefficient.

Figure 2d illustrates a simple MINLP example, where x_1 is an integer variable ranging from 0 to 9, and x_2 is a continuous variable. The cost function is nonlinear and exhibits multiple local optima. Figure 2e presents the discrete matrix analogue of the continuous cost function. We approximate the function in TT format with rank $r_{\max} = 2$, as shown in Figure 2f. The results indicate that even with a low TT rank, TT-Cross can identify high-quality local optima, demonstrating the strong modeling and optimization capabilities of TT. However, the results obtained by TTGO do not correspond to the global optimum, highlighting that a low-rank TT approximation may fail to fully capture the complexity of the original function. In such cases, TTTS leverages strategic search to efficiently converge to the global optimal solution within finite time.

Inverse kinematics

We consider a standard inverse kinematics (IK) task, where the objective is to compute a collision-free configuration of a robot manipulator such that the end-effector reaches a desired target pose. This corresponds to a single-stage, one-step optimization problem (i.e., $T = 1$ and $K = 1$ in (1)) with continuous decision variables \mathbf{u} , subject to kinematic and collision constraints. The objective function minimizes task-space error, which penalizes deviations between the end-effector pose and the desired target. Additional constraints include joint limits, collision avoidance, and reachability. Despite its simple definition, this task serves as a meaningful testbed featuring nonlinear kinematics and nonconvex constraints, making it well-suited to evaluate the effectiveness of TT in enabling efficient tree search.

We conducted ablation study to analyze the necessity of each component of TTTS, which consists of three main components: TT-Tree Initialization, TT-Tree Search, and TT-Tree Refinement. TT-Tree Initialization typically requires some computation time due to TT-Cross approximation (particularly for high-dimensional systems), but this process is performed offline. At this step, the state space is augmented with task variables, enabling rapid task-conditioned retrieval for TT-Tree Search. In our experiments, we set $r_{\max} = 21$ for both 3-DOF and 7-DOF manipulators, resulting in a coarse approximation of the full decision tree. Notably, obstacle avoidance tends to introduce

high-rank behavior, making low-rank TT approximations less accurate. As shown in Figure 3 (A), TT-Tree Initialization alone does not yield the global optimum, highlighting the limitations of using TT approximation by itself. However, after performing TT-Tree Search and Refinement, the final task-space error is zero, indicating that the globally optimal solution was successfully found.

A Ablation Study for Inverse Kinematics									
	TT-Tree Init. (Offline)		TT-Tree Search		TT-Tree Refine.				
	Error	Time (s)	Error	Time (s)	Error	Time (s)			
3-joint	0.02 ± 0.01	0.28	0.02 ± 0.01	0.05 ± 0.00	0.00 ± 0.00	0.08 ± 0.00			
7-joint	0.21 ± 0.10	0.65	0.10 ± 0.06	0.22 ± 0.02	0.00 ± 0.00	0.31 ± 0.00			

B Ablation Study for Motion Planning									
	TT-Tree Init. (Offline)			TT-Tree Search			TT-Tree Refine.		
	Error	Total Cost	Time (s)	Error	Total Cost	Time (s)	Error	Total Cost	Time (s)
3-joint	0.13 ± 0.06	7.42 ± 3.97	5.50	0.13 ± 0.06	7.41 ± 3.98	0.08 ± 0.05	0.00 ± 0.00	0.41 ± 0.49	0.31 ± 0.00
7-joint	0.06 ± 0.03	3.64 ± 1.54	1.27	0.05 ± 0.03	3.08 ± 1.43	0.10 ± 0.03	0.00 ± 0.00	0.11 ± 0.04	0.34 ± 0.00

C Ablation Study for Face-switching Planar Pushing									
	TT-Tree Init. (Offline)			TT-Tree Search			TT-Tree Refine.		
	Error	Total Cost	Time (s)	Error	Total Cost	Time (s)	Error	Total Cost	Time (s)
	0.19 ± 0.05	0.16 ± 0.02	4.85	0.08 ± 0.03	0.11 ± 0.03	0.09 ± 0.03	0.00 ± 0.00	0.06 ± 0.00	0.03 ± 0.00

Figure 3: Ablation studies for diverse robotics tasks. (A) Ablation study for inverse kinematics. (B) Ablation study for motion planning. (C) Ablation study for face-switching planar pushing.

Motion planning around obstacles

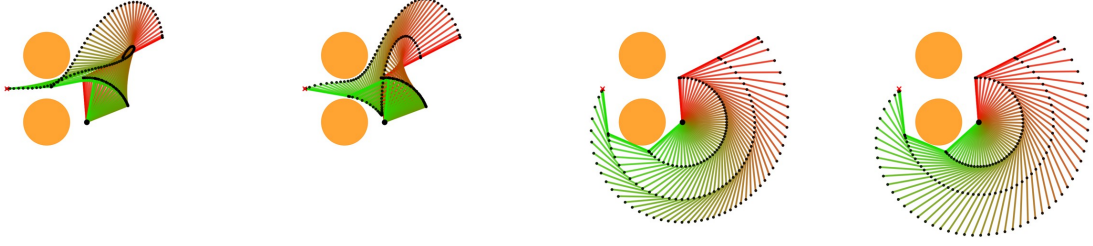
We apply our framework to a motion planning problem in which a robot must generate a smooth, collision-free trajectory from a given start to a goal configuration. The problem is formulated over T time steps, where the continuous trajectory is represented using basis functions as $\mathbf{u}^{[T]} = \sum_{b=1}^B \mathbf{\Psi}^b \mathbf{w}^b$, and the optimization variables are the corresponding weights $\{\mathbf{w}^b\}_{b=1}^B$. The objective is to minimize a cost function that encourages smooth motion (e.g., penalizing velocity or acceleration), while ensuring accurate goal reaching. The constraints include joint limits and collision avoidance with static obstacles.

Figure 4 (A) presents our first test scenario: a 3-joint manipulator reaching task. This task is particularly challenging because the target lies on the opposite side of the robot, with two circular obstacles obstructing the direct path. The trajectories found by our approach exhibit multiple solution modalities under the same initial configuration and target. Notably, the first two trajectories shown in the figure require the manipulator to initially move away from the target and then pass through a narrow passage between the obstacles, which is not easy to find and requires long-horizon anticipation. This setting involves numerous local optima and a narrow feasible solution space, necessitating long-horizon planning rather than short-horizon control. The results illustrate our framework’s ability to overcome local optima and support long-term decision-making. We further applied our approach to a 7-joint manipulator. The robot arm must move its end-effector from one level of the shelf to another while avoiding obstacles, such as the shelf frame, across its entire body surface. This setup is representative of daily tasks such as pick-and-place or bookshelf arrangement. Figure 1 (B) shows the resulting trajectories, where end-effector paths are visualized as curves. Different colors indicate distinct solutions discovered by the algorithm.

Figure 3 (B) presents the ablation study of our approach applied to motion planning (MP) problems. As the three stages of TTTS are applied, both the final state error and the total trajectory cost consistently decrease, demonstrating the effectiveness of each component. The final errors for both tasks are zero, indicating that a collision-free joint trajectory was successfully found to reach the target. An interesting observation is that TT-Tree Initialization takes longer for task *MP1* than for *MP2*, as *MP1* is a more challenging problem with more local optima. Accordingly, we set $r_{\max} = 41$ for *MP1* and $r_{\max} = 21$ for *MP2*. The TT approximation in *MP1* achieves high accuracy, and further iterations of TT-MCTS provide limited improvement. This suggests that, with sufficient storage capacity, we can use higher TT ranks for more accurate tree approximation, accelerating online inference. In contrast, the results of *MP2* highlight the effectiveness of TTTS under limited storage conditions, where low-rank approximations still capture informative representations of complex decision trees. By combining low-rank approximation with the strong exploration capability of MCTS, TTTS ensures convergence to the bounded global optimum.

A

3-joint Manipulator Motion Planning



B

Face-switching Planar Pushing

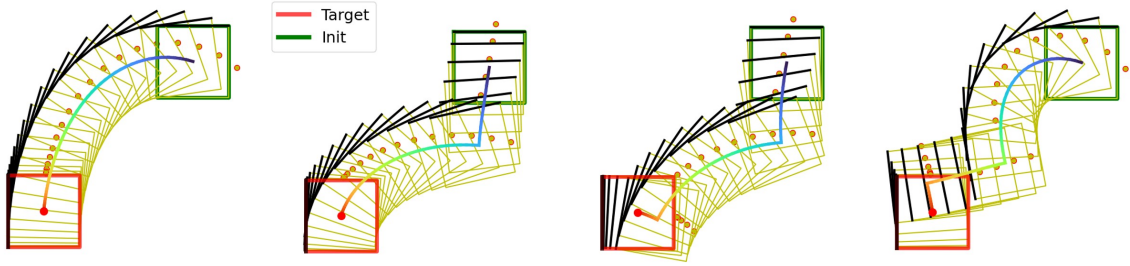


Figure 4: Multimodal solutions for motion planning around obstacles and face-switching planar pushing. (A) 3-joint manipulator motion planning with multimodal solutions. The trajectory is visualized using a red-to-green color spectrum to indicate temporal evolution. (B) Face-switching planar pushing task with multimodal solutions. Given the same initial configuration $[0.25, 0.25, -\frac{\pi}{2}]$ and target $[0.25, 0.25, -\frac{\pi}{2}]$, our algorithm can find multimodal solutions to accomplish the task, by jointly optimizing over discrete contact faces and continuous motion variables. The black edge of the rectangle indicates the cube's orientation.

Multi-stage motion planning

Multi-stage motion planning encompasses a broad class of realistic robotic problems, such as multi-stage forceful manipulation (29) and multi-primitive sequencing (30). The objective is to generate a trajectory that enables a robot to interact intelligently with its environment, typically involving contact mode switches (e.g., sticking, sliding, or transitioning between different manipulation primitives). In this article, the trajectory is parameterized by a sequence of basis weights \mathbf{w}_k , such that the continuous state at each stage is given by $\mathbf{u}_k = \mathbf{\Psi}_k \mathbf{w}_k$. Discrete modes m_k represent different contact or task-specific phases. The optimization aims to minimize a total cost consisting of smoothness penalties, control effort, and task-specific objectives, while satisfying constraints such as collision avoidance, dynamics, and mode transitions.

We use face-switching planar pushing (31) as a representative task, in which a robot must push a cube from an initial configuration to a target configuration, while accounting for underactuated dynamics and face-switching mechanisms. The robot must determine the end-effector velocity (continuous) and which face to establish contact (discrete). This task is particularly challenging due to the nonlinear dynamics and the hybrid nature of the decision variables, which present difficulties for both gradient-based and sampling-based optimization methods. The goal of this experiment is to demonstrate the ability of our approach to efficiently handle such hybrid decision-making problems, coupled with nonlinear dynamics. Figure 4 (B) illustrates the found cube trajectories given the same initial and target configuration, showcasing the multimodal nature of the solutions. The number of face switches varies from 0 to 2, along with diverse, smooth continuous trajectories.

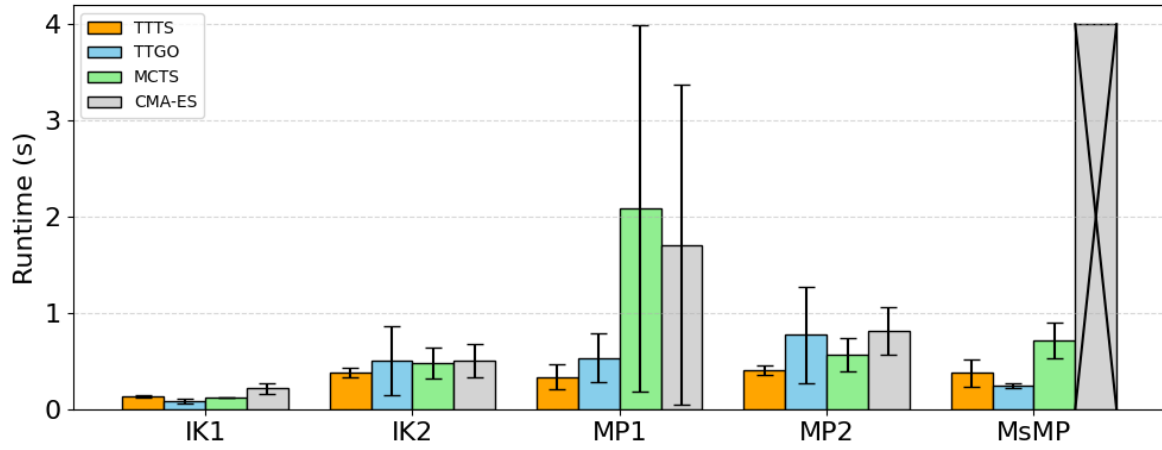
Figure 3 (C) presents the ablation study for this task. The TT approximation of the decision tree is obtained with a rank setting of $r_{\max} = 41$. The results show that the TT approximation alone is not sufficiently accurate to capture the full landscape of the objective function. However, the subsequent tree search significantly improves the solution quality, and the final refinement step enables convergence to the global optimum. An interesting observation is that, compared with the policy learning formulation (i.e., infinite-horizon dynamic programming) proposed in (32,33), this finite-horizon planning formulation requires a significantly higher TT rank to accurately represent the objective function. This is because trajectory-level planning uses decision variables (i.e., basis weights) that influence the entire trajectory, where small changes can induce large,

structured variations, necessitating higher representational capacity to capture complex temporal dependencies. This further motivates the necessity of combining TT approximation with tree search, rather than relying on TT alone.

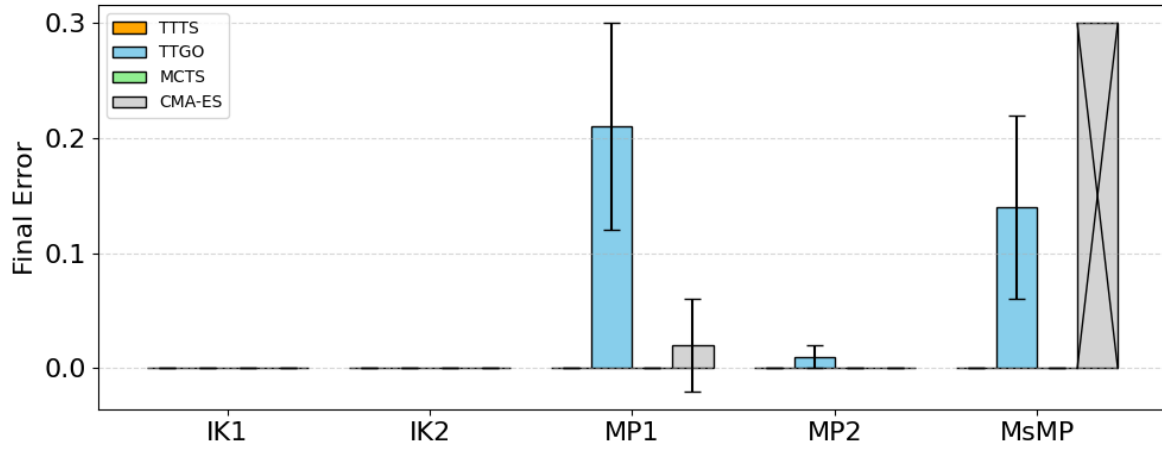
Numerical comparisons

We further compare our proposed approach with several baselines for solving the aforementioned problems, including TTGO, MCTS, and CMA-ES. Both TTGO and MCTS provide valuable insights that inspire our method, and each can be considered a special case of TTTS. TTGO samples solutions directly from the TT approximation, which can result in repeated sampling of the same solutions. In contrast, our approach incorporates the strategic search capability of MCTS, which ensures global convergence. CMA-ES is a state-of-the-art sampling-based optimization technique that does not rely on gradient information, allowing it to avoid poor local optima. This makes it suitable for many robotic optimization problems involving nonlinear dynamics or obstacle avoidance.

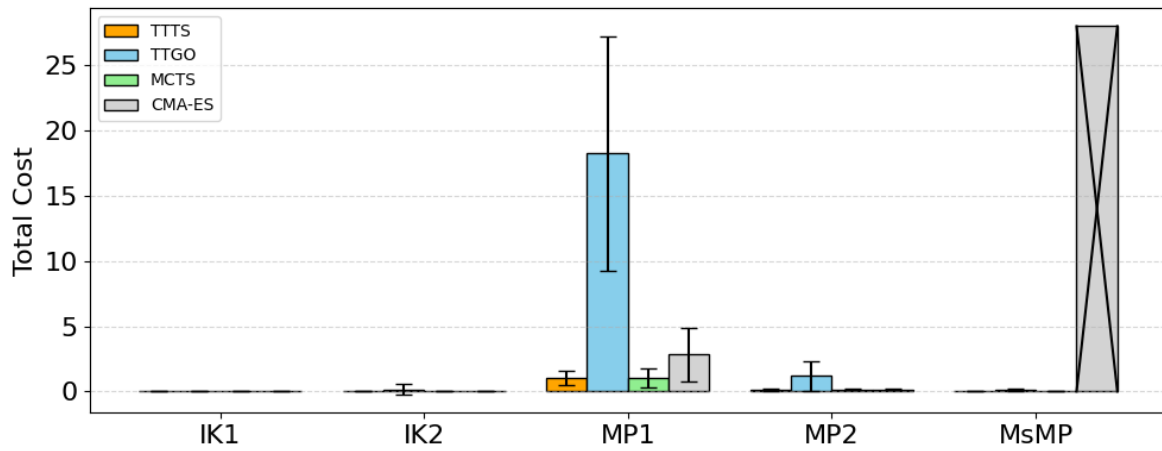
Figure 5 compares runtime, final state error, and total trajectory cost across these methods. From Figures 5c and 5b, we observe that TTTS achieves results comparable to MCTS when the latter is given sufficient time, highlighting its ability to reach similar global convergence. Figure 5a further shows that TTTS requires significantly less computation time. TTGO performs well for most tasks and is highly efficient in terms of computation time, but it struggles in *MPI* due to the complex cost landscape, where low-rank TT approximation is insufficient to capture all necessary features. In contrast, TTTS leverages strategic tree search to explore the decision space more effectively, achieving global convergence in finite time. Additionally, the sampling-based refinement in TTTS improves solution quality over the gradient-based refinement used in TTGO, especially in nonconvex settings. CMA-ES performs well on most tasks, but fails in *MPI* and *MsMP*. In *MPI*, a narrow passage between obstacles challenges the single-modality evolution strategy, causing it to become trapped in local optima. For *MsMP*, which involves both discrete and continuous decision variables, CMA-ES is not applicable (indicated by diagonal hatching in the bar chart). These experiments highlight the computational efficiency of TTTS, enabled by the TT approximation of the decision tree, and its global convergence properties, enabled by the compact representation of TT and the



(a) Runtime Comparison



(b) Final state error comparison



(c) Total cost comparison

Figure 5: Performance Comparison of TTTs, TTGO, CMA-ES and MCTS. The diagonal connections in the bar chart indicates the incompatibility of CMA-ES on *MsMP*.

strategic search adopted from MCTS.

Model Predictive Control for bimanual whole-body manipulation

We evaluate our approach using a Model Predictive Control (MPC) formulation applied to a bimanual whole-body manipulation task. This task is particularly challenging due to complex contact dynamics between objects, the whole-body geometry of the robot, and interactions with the environment, all of which make accurate modeling difficult. Physical simulators such as MuJoCo (34) and IsaacGym (35) can help address these challenges. However, the resulting sim-to-real gap necessitates the use of real-time MPC. Given the simulator as a black-box forward dynamics model, sampling-based MPC becomes a promising approach, as it does not rely on explicit gradient information. Nevertheless, such methods often suffer from high sample complexity and slow convergence, limiting their practicality for real-world deployment. In this experiment, we aim to demonstrate that TTTS can quickly find high-quality solutions to support real-time, sampling-based MPC. Specifically, we use Genesis (36) as the simulator due to its parallel simulation capabilities, and the number of environments is set to 500.

Figure 6 illustrates the performance differences between TTTS, TTGO, MCTS, and CMA-ES. The computation time is limited to 1 second. A task is considered successful if the angular error at the final timestep satisfies $|\theta - \theta^*| < 3^\circ$, where θ is the object’s final z-axis orientation and θ^* is the desired target angle. We evaluate five randomly generated configurations and report success rate, final state error, and total trajectory cost. TTGO achieves a decent success rate with a low TT rank ($r_{\max} = 10$), but its limited accuracy leads to occasional failures. MCTS offers theoretical global convergence but requires more time, making it impractical for real-time MPC. CMA-ES also performs poorly due to slow convergence. In contrast, TTTS first approximates the decision tree in TT format, which accelerates convergence toward promising regions. It then performs a TT-based tree search, enabling efficient exploitation and strategic exploration. The results, including final error and total cost, confirm the effectiveness of TTTS in supporting real-time MPC for contact-rich manipulation.

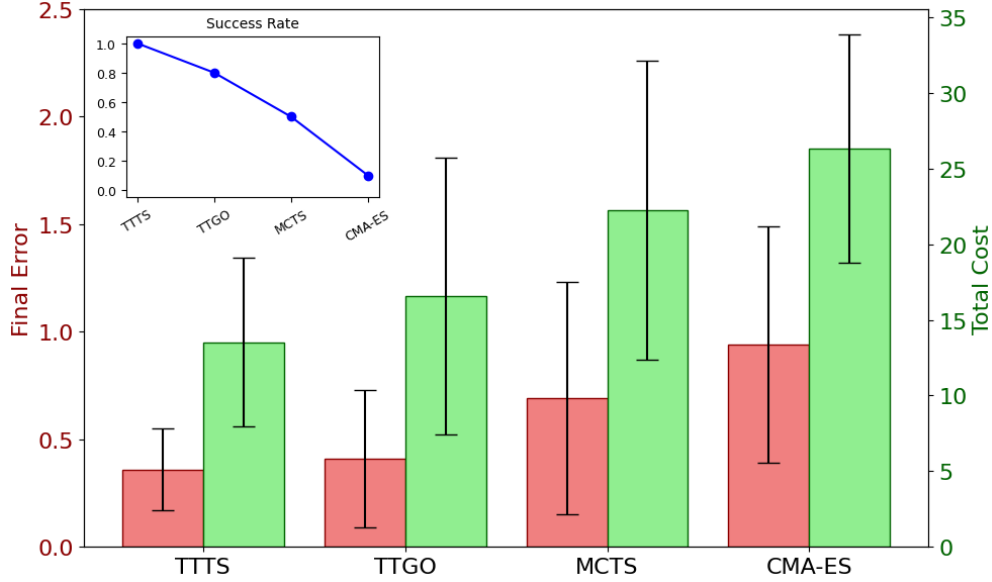


Figure 6: Comparison for bimanual whole-body manipulation. The red bars represent the final state error achieved by different methods, while the green bars correspond to the total cost.

Real-world experiments

We validated our approach in the real world through the whole-body bimanual manipulation task. Two 7-DoF Franka robots and a RealSense D435 camera were used. The manipulated object was a large box with the size of $36\text{cm} \times 26\text{cm} \times 34\text{cm}$, which is representative of objects commonly found in warehouse applications. The task was to rotate the box to a target orientation and then lift it. It involved complex contact interactions among the robots, the object, and the table, as well as the full-body surface geometry of the two robot arms, making the system particularly difficult to model.

To address this, we used Genesis to predict the box trajectory given a sequence of control commands, eliminating the need to manually model the complex system dynamics. We first applied TT-Cross to obtain a low-rank TT approximation, augmented with the object pose. During execution, we conditioned on the current object pose and performed tree search for 3 iterations, which typically produced effective results thanks to the guidance provided by the TT approximation.

At each time step (every 1 second), we generated a 9-second trajectory in a model predictive control (MPC) manner to bridge the sim-to-real gap. Figure 7 presents keyframes of one task of rotating the box for 90° . We can observe that the robots geometry is actively utilized to establish

contacts with the object, enabling whole-body bimanual manipulation. More tasks are demonstrated in the accompanying video.

Discussion

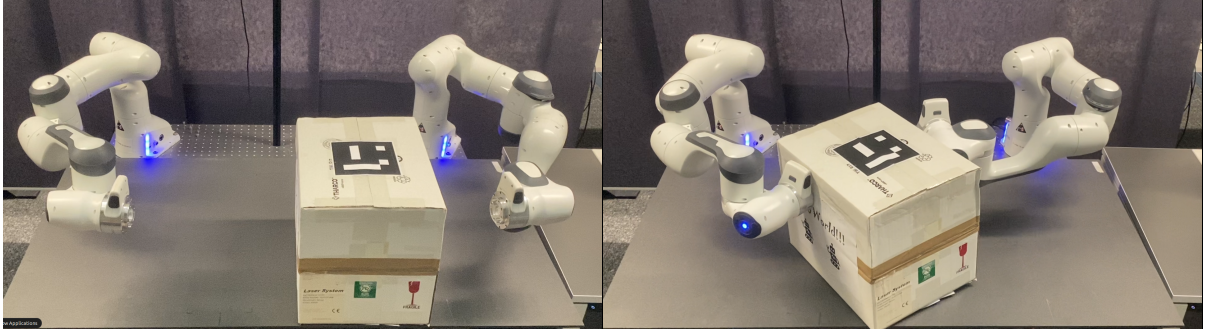
Qualitative comparison with existing algorithms

Gradient-based Methods

Gradient-based and Newton-based methods (i.e., first and second-order optimization) are the most popular approaches in robot optimization, characterized by rapid convergence when gradients of the objective and constraints are available, when suitable initial guesses are provided. Standard methods include Differential Dynamic Programming (DDP) (37, 38), iterative Linear Quadratic Regulators (iLQR) (39), and trajectory optimization frameworks such as CHOMP (40) and TrajOpt (41). The main advantage of gradient-based and Newton-based optimization is its efficiency in smooth and convex problem formulations, enabling practical deployment in real-time robot control scenarios. In these applications, gradients and Hessians provide useful local guidance, significantly speeding up convergence.

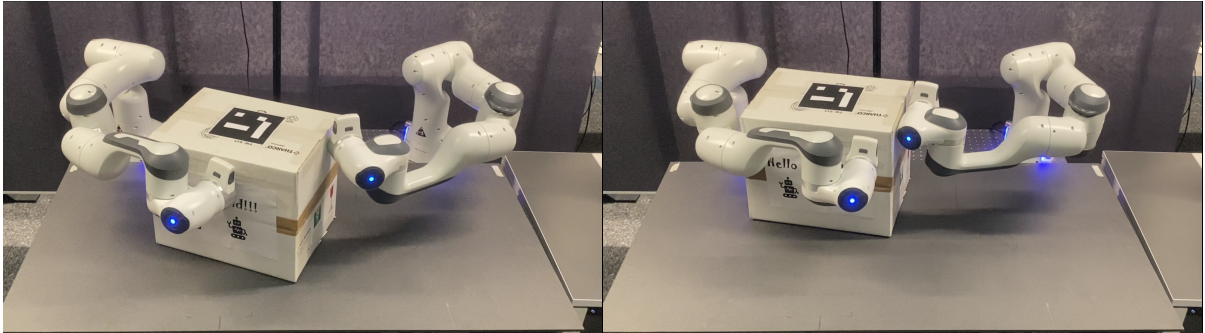
However, the critical limitation of gradient-based and Newton-based methods arises in scenarios involving highly nonlinear, non-convex cost landscapes or discontinuous constraints, such as hybrid modes, contacts, and collision avoidance conditions (7, 15). These scenarios are often too sensitive to initialization and often get trapped in poor local minima, demanding accurate initial guesses or sophisticated initialization schemes.

In contrast to these approaches, TTTS does not rely on convex structures and/or initial guesses. It can address highly nonlinear, non-convex cost landscapes, as well as mixed-integer decision variables. For example, the planar pushing task with face switching mechanism requires optimization on both discrete and continuous decision variables, which is not solvable with typical gradient-based and Newton-based methods. TTTS tackles this problem through TT approximation and strategic tree search, where gradient-based approach can still be integrated within the framework as a refinement step for continuous variables, which limits the impact of domain discretization that the approach requires by enabling a coarse-to-fine optimization scheme.



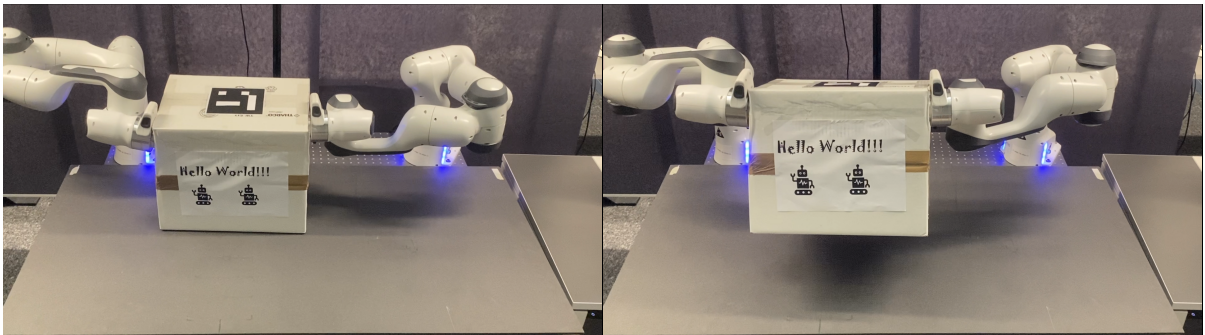
(a)

(b)



(c)

(d)



(e)

(f)

Figure 7: Keyframes of bimanual whole-body manipulation. The system is initialized as (a), and the objective is to rotate the box 90° and then lift it as (f). We can observe that the robots can actively exploit whole-body geometry to make and break contacts with the object, completing the overall task successfully.

Sampling-based Methods

Sampling-based methods, including Rapidly-exploring Random Trees (RRT) (8) and Probabilistic Roadmaps (PRM) (9), complement gradient-based approaches by leveraging random exploration of the search space. Their primary advantage lies in their ability to handle complex constraints, discontinuities, and high-dimensional state spaces without explicit gradient information. Variants like RRT* (42), BIT* (43) and CMA-ES (44) further improve path optimality and convergence rates, demonstrating remarkable flexibility and scalability in challenging environments.

Nevertheless, sampling-based methods typically suffer from slow convergence when dealing with narrow passages or high-dimensional solution space, as their success heavily depends on the probabilistic coverage of critical regions in the search space (42, 45). Consequently, they often require extensive computational resources or advanced heuristic-guided sampling strategies to achieve satisfactory performance. Moreover, sampling-based methods can only ensure probabilistic completeness, lacking a strategical sampling behavior for global convergence, thus making solution finding not guaranteed in finite time.

In contrast, TTTS leverages TT approximation to quickly explore the full tree, playing as informative priors. It also possesses strategical search for solution finding, leading to global convergence in finite time. For example, as shown in the 3-joint motion planning task, CMA-ES suffers from the narrow passage, while TTTS can effectively find the multi-modal solutions. In our framework, CMA-ES is integrated in TTTS for refinement of the TT-Tree search solutions to bridge the gap between continuous decision domain and discretized solution.

Search-based Methods

Search-based planners, such as A* (10) and Monte Carlo Tree Search (MCTS) (46), formulate the optimization problem explicitly as a discrete search through structured state or state-action spaces (10, 47). A major advantage of these methods is their strong theoretical guarantees of completeness and optimality (given suitable heuristics), particularly valuable in environments with discrete or easily discretizable action sets. Furthermore, methods like MCTS effectively balance exploration and exploitation, significantly improving planning efficiency in complex domains (48).

However, search-based methods typically require discretizing continuous spaces, leading to

exponential growth in computational complexity as dimensionality increases (aka. curse of dimensionality). The discretization itself introduces approximation errors and scaling issues, rendering these approaches less effective or computationally prohibitive in high-dimensional continuous domains without carefully designed discretization schemes or heuristics (49). Rivière *et al.* addresses this issue by decomposing continuous dynamical systems through the spectrum of the locally linearized controllability Gramian (22), but the discretization is achieved through local linearization, which can still lead to node explosion for highly nonlinear dynamical systems, such as robot manipulators.

TTTS adopts the strategical search behavior from MCTS to ensure global convergence, and it leverages TT to reduce the combinatorial complexity into linear complexity for both storage space and computation time. The TT approximation provides effective guidance for efficient tree search and enables parallel rollouts for faster convergence.

Hybrid Methods

To overcome the limitations of purely gradient-based, sampling-based, or search-based methods, hybrid approaches have been developed that integrate multiple planning paradigms. For example, combining trajectory optimization with sampling-based planners (such as RRT followed by trajectory optimization (50)) enables more effective exploration in high-dimensional spaces. In the context of mixed-integer programming, approaches like Logic-Geometric Programming (LGP) (3) alternate between discrete symbolic search and continuous geometric optimization. More recent hybrid methods combine global search strategies (e.g., MCTS or heuristic-based planners) with local refinement techniques or learning-based value estimation (51, 30). These approaches have proven especially effective for solving complex planning problems that involve both discrete and continuous variables (52, 53). By leveraging the strengths of both local optimization and global search, these methods achieve practical efficiency across a wide range of applications, including manipulation, legged locomotion, and multimodal task planning.

Despite these benefits, hybrid methods often require careful engineering and tuning of parameters to balance computational resources effectively. Additionally, the integration of different planning paradigms introduces additional algorithmic complexity and implementation overhead, complicating both theoretical analysis and practical deployment.

TTTS can be seen as a hybrid approach that combines global search with local refinement, but different from the vanilla combination, TT provides a novel representation of decision tree, enabling more efficient and parallelizable tree search. Moreover, different from the hierarchical structure that alternates between high-level discrete search and low-level continuous optimization, TTTS addresses the mixed-integer optimization jointly, by considering a joint distribution.

Materials and Methods

In this section, we first present a general formulation that encompasses a wide range of robotic tasks. We then introduce the proposed algorithm, which leverages Tensor Train (TT) factorization for efficient Monte Carlo Tree Search (MCTS). Finally, we provide a theoretical analysis demonstrating convergence to the global optimum.

Problem formulation

We consider a general robot optimization formulation that can address diverse problems, such as inverse kinematics, motion planning, multi-stage motion planning with mode switching, and model predictive control, which corresponds to a large sets of mathematical programs, including nonlinear programming (NLP), large-scale (aka. high-dim) NLP and mixed-integer nonlinear programming (MINLP). In particular, we leverage basis functions to reduce the dimensionality for large-scale NLP formulation.

We describe here the notation and variables:

K	the number of discrete modes (a.k.a. stages).
$m_k \in \mathcal{M}$	the discrete <i>mode</i> (or discrete decision variable) at stage k , chosen from some finite (or countable) set \mathcal{M} .
$\mathbf{x}_k^t \in \Omega_{\mathbf{x}} \subseteq \mathbb{R}^n$	a continuous state (or configuration) at stage k at time t .
$\mathbf{u}_k^t \in \Omega_{\mathbf{u}} \subseteq \mathbb{R}^p$	a continuous control input at stage k at time t .
T	trajectory length for each stage.
B	number of basis functions.
$\Psi_k \in \mathbb{R}^{T \times B}$	a chosen set of basis functions for stage k , which is used to reconstruct the continuous decision variable from weights.
$\mathbf{w}_k \in \Omega_{\mathbf{w}} \subseteq \mathbb{R}^B$	the vector of basis <i>weights</i> at stage k . Hence we let $\mathbf{u}_k^{[T]} = \Psi_k \mathbf{w}_k$, which encodes the continuous variables in terms of basis representations.
$c(m_k, \mathbf{x}_k, \mathbf{u}_k)$	stage cost (e.g., energy, distance, penalty) for k .
$c_{\text{terminal}}(m_K, \mathbf{x}_K^T)$	terminal cost, e.g. capturing the final configuration error.
$\phi(\cdot) \leq 0, \psi(\cdot) = 0$	general inequality/equality constraints that can represent kinematic limits, collision avoidance, robot dynamics, or boundary conditions.

Note that we use a bracket subscript to indicate a sequence, e.g., $\mathbf{x}_k^{[T]}$ represents the full trajectory at stage k , and $\mathbf{u}_{[K]}^{[T]}$ represents the control variables including the complete long-horizon trajectory. The unified mathematical formulation for our robot optimization problems is:

$$\min_{m_{[K]}, \mathbf{u}_{[K]}^{[T]}} \sum_{k=0}^K \int_0^T c(m_k, \mathbf{x}_k^t, \mathbf{u}_k^t) dt + c_{\text{terminal}}(m_K, \mathbf{x}_K^T) \quad (1)$$

$$\text{s.t. } \mathbf{u}_k^{[T]} = \sum_{b=0}^B \Psi_k^b \mathbf{w}_k^b, \quad (2)$$

$$\forall_{k=0}^K \quad m_{k+1} \in \text{succ}(m_k, \mathbf{x}_k^{[T]}, \mathbf{u}_k^{[T]}), \quad (3)$$

$$\forall_{k=0}^K \quad \phi(m_k, \mathbf{x}_k^{[T]}, \mathbf{u}_k^{[T]}) \leq 0, \quad (4)$$

$$\forall_{k=0}^K \quad \psi(m_k, \mathbf{x}_k^{[T]}, \mathbf{u}_k^{[T]}) = 0, \quad (5)$$

$$(m_0, \mathbf{x}_0^0) = (m_{\text{init}}, \mathbf{x}_{\text{init}}), \quad (6)$$

where:

- (2) encodes the full trajectory of decision variables using basis functions.

- (3) enforces allowed transitions m_{k+1} in the discrete mode set \mathcal{M} given the current mode m_k and the system trajectory $\mathbf{x}_k^{[T]}, \mathbf{u}_k^{[T]}$.
- (4) and (5) represent the system dynamics, consistency of different modes, and other physical constraints.
- m_{init} and x_{init} denote the initial mode and state.

This formulation unifies many problems in robotics, including:

Inverse Kinematics (IK) For a basic IK problem, we can set $T = 1, B = 1$ and have only a single mode $K = 1$. The joint configuration $\mathbf{u}_1 = \mathbf{\Psi}_1 \mathbf{w}_1$ describes the joint configuration, namely

$$\min_{\mathbf{w}_1} c(\mathbf{\Psi}_1 \mathbf{w}_1) \quad \text{s.t.} \quad \phi(\mathbf{\Psi}_1 \mathbf{w}_1) \leq 0, \quad \psi(\mathbf{\Psi}_1 \mathbf{w}_1) = 0,$$

where c could measure the end-effector pose error relative to a target, and ϕ, ψ encode joint limits, collision avoidance, etc.

Motion Planning (MP) For a typical MP problem, we can set $K = 1$ to ensure there is only a single mode. The trajectory length is T , and the decision variables are the weights \mathbf{w} for the basis function encoding.

Multi-stage Motion Planning (MsMP) For a multi-stage planning problem with multiple discrete contact modes (e.g. foot placements or manipulation primitives) and continuous joint trajectories, we use K to represent the number of overall stages. At each stage k :

$$m_k \in \mathcal{M}, \quad \mathbf{u}_k^{[T]} = \mathbf{\Psi}_k \mathbf{w}_k.$$

The constraints ensure collision-free motion, piecewise dynamics, and valid contact transitions among modes. The task is to find both the discrete mode sequence $m_{[K]}$ and the continuous motion trajectory $\mathbf{u}_{[K]}^{[T]}$.

Monte Carlo Tree Search

Equation (1) presents a general formulation that covers many optimization problems in robotics. However, it results in a Mixed-Integer Nonlinear Programming (MINLP) problem, which remains

NP-hard (54). Due to the presence of non-convex constraints and the joint optimization over discrete and continuous variables, both gradient-based and sampling-based approaches face significant challenges. Monte Carlo Tree Search (MCTS) emerges as a powerful tool for tackling such problems through strategic exploration of the solution space.

MCTS begins at the root and selects a promising node at each layer by balancing exploitation and exploration, typically via an upper confidence bound:

$$i_{[j]} \leftarrow \arg \max_{i_{[j]} \in \Omega}^k \left(\frac{w_{i_{[j]}}}{v_{i_{[j]}}} + c \sqrt{\frac{\log v_{i_{[j-1]}}}{v_{i_{[j]}}}} \right), \quad (7)$$

where j denotes the current depth in the tree, and $i_{[j]} = (i_1, i_2, \dots, i_j)$ represents the complete sequence from the root to the selected node. Here, $w_{i_{[j]}}$ and $v_{i_{[j]}}$ denote the cumulative reward and visit count of the terminal node in path $i_{[j]}$, while $v_{i_{[j-1]}}$ refers to the visit count of its parent. The constant c regulates the trade-off between exploration and exploitation.

After selection, MCTS expands the chosen node by generating a new child, followed by a simulation stage in which a rollout policy estimates the outcome from that child. The simulation results are then propagated back through the visited nodes, updating their value estimates and visit counts to guide subsequent searches. Through strategic exploitation and exploration, MCTS can efficiently explore large search spaces and asymptotically converge to the global optimum.

To support strategic search behavior, it is essential to store and update the value and visit count for each node. This leads to a combinatorial complexity of $\mathcal{O}(N^d)$ in both computation time and memory usage, where N is the number of nodes per layer and d is the depth of the tree. Such complexity severely limits the applicability of MCTS in many tasks.

Tensor Factorization for MCTS

We introduce TT as an efficient representation for decision trees that significantly reduces combinatorial complexity to linear complexity. A multi-layer decision tree can be represented as a high-dimensional tensor \mathbf{T} , where each complete branch corresponds to a particular element within \mathbf{T} , and the element indices correspond to the sequence of node indices along that branch. As illustrated in Fig. 8 (A), the two representations are equivalent. For instance, a decision tree with d layers and N nodes per layer corresponds to a tensor of size N^d . If the optimal solution in the tree is

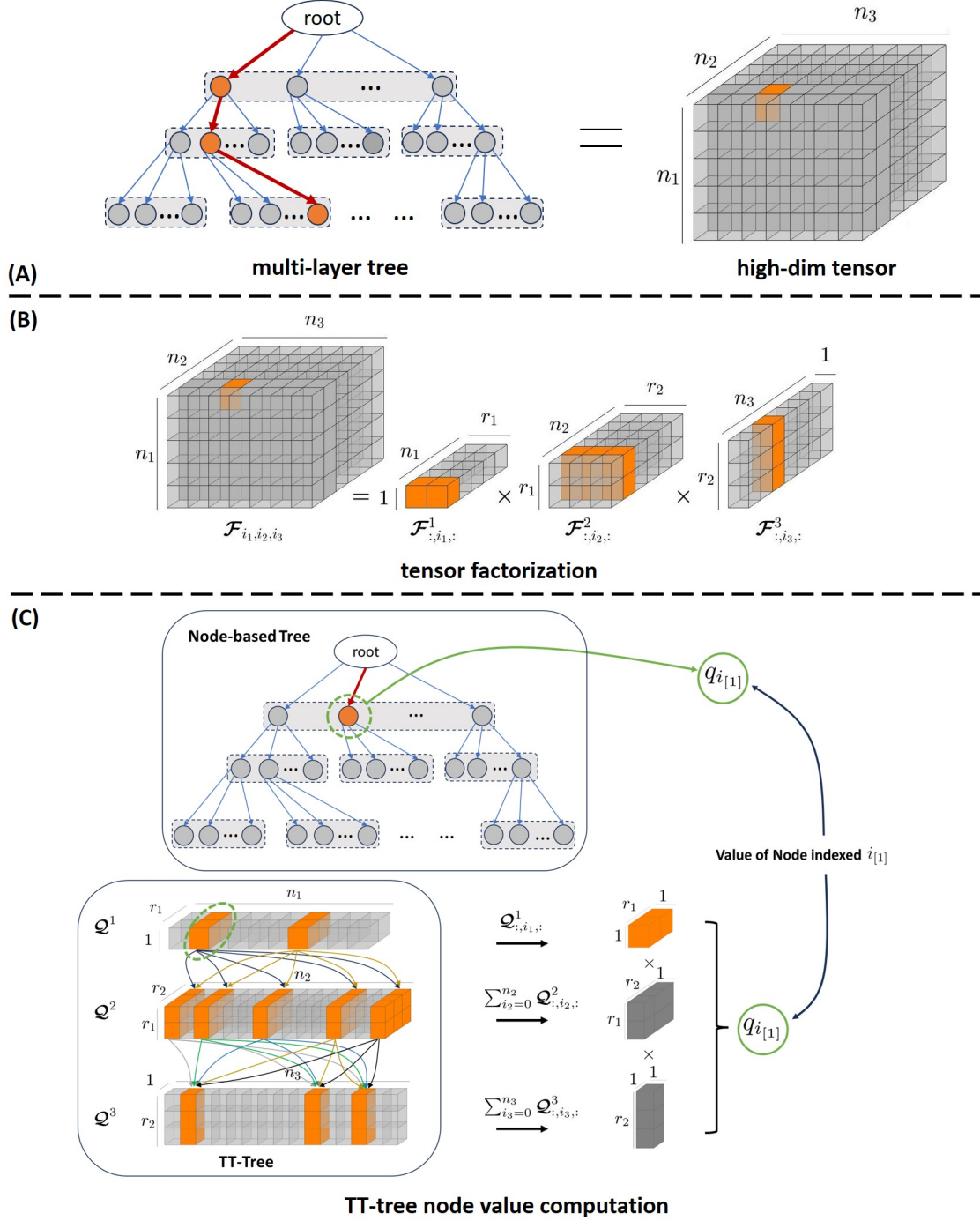


Figure 8: Tree-Tensor-TT transformation. (A) A multi-layer decision tree can be equivalently represented as a high-dimensional tensor, where each tensor element corresponds to the value at the terminal node of a branch. (B) Tensor decomposition in TT format. A 3-dimensional tensor can be represented using three third-order TT cores. (C) Node value computation given a tree in TT format. This example illustrates how the value of a node in the first layer is computed using TT cores.

indexed by (i_1, i_2, \dots, i_d) , where i_k denotes the node index at the k -th layer, then the corresponding optimal tensor entry has the same index.

To reduce this combinatorial complexity, our objective is to express the tree with linear complexity $\mathcal{O}(\lambda Nd)$, where λ is a scaling factor. This is equivalent to representing a high-dimensional tensor of size $\mathcal{O}(N^d)$ using a compact, low-rank decomposition, which is a well-studied problem in numerical mathematics (55). Specifically, we employ TT to exploit the separable structure and reduce inter-layer dependencies. As a result, the original high-dimensional tensor can be efficiently represented using significantly fewer parameters through a sequence of third-order cores, namely:

$$\mathbf{T}_{(i_1, \dots, i_d)} \approx \mathcal{T}_{:,i_1,:}^1 \mathcal{T}_{:,i_2,:}^2 \cdots \mathcal{T}_{:,i_d,:}^d, \quad (8)$$

where \mathcal{T}^j is the core corresponding to the j -th dimension (i.e., the j -th layer of the tree). Figure 8 (B) presents an illustrative example of a three-dimensional tensor.

Algorithm 1 presents the pseudocode of the proposed method. As indicated in (7), a key component of MCTS is its ability to perform strategic search by leveraging the value and visit count information stored at each node in the tree, denoted by \mathbf{Q} and \mathbf{V} , respectively. We utilize TT to efficiently store this information, represented as \mathcal{Q} and \mathcal{V} .

To initialize the search, TT-Cross is first employed to approximate the decision tree using a low-rank TT model, augmented with conditional variables (e.g., task parameters or initial states), resulting in a conditional model $\tilde{\mathcal{Q}}$. Given a set of condition variables \mathbf{z} , the value tensor is instantiated as $\mathcal{Q} = \tilde{\mathcal{Q}}(\mathbf{z})$. Owing to the *maximum volume* principle used in TT-Cross, the resulting TT model typically captures representative features of the decision tree, enabling the identification of promising branches from the very first iteration. The visit count tensor \mathcal{V} is initialized to zero.

The algorithm then follows the standard MCTS pipeline: selection, expansion, simulation, and backpropagation. Due to dependence on the parent nodes, the value and visitation statistics of a node are path-dependent, introducing non-Markovian behavior. Querying the value of node $n_{i_{[j]}}$ requires summing over all completions of the branch from layer $j + 1$ to depth d . Given the full tree approximated in TT format, the value of a node at level j , denoted as $q_{i_{[j]}}$, can be efficiently

computed by

$$\begin{aligned}
q_{i_{[j]}} &= \sum_{i_{j+1}=0}^{N_{j+1}} \cdots \sum_{i_d=0}^{N_d} \mathbf{Q}_{(i_1, \dots, i_j, i_{j+1}, \dots, i_d)} \\
&\approx \sum_{i_{j+1}=0}^{N_{j+1}} \cdots \sum_{i_d=0}^{N_d} \mathbf{Q}_{:,i_1,:}^1 \cdots \mathbf{Q}_{:,i_j,:}^j \cdots \mathbf{Q}_{:,i_d,:}^d,
\end{aligned} \tag{9}$$

where each TT core \mathbf{Q}^l encodes the factorized structure of the tree at layer l . To compute the node value at depth j , we extract the corresponding slices from the first j TT cores (representing the visited layers), and perform summation over indices in the remaining cores from $j+1$ to d . The final node value is obtained by multiplying the resulting matrices across all layers. Figure 8 (C) illustrates how to compute the value of a node in the first layer of a three-layer tree using TT cores. The multiple arrows between TT cores indicate the ability to perform parallel selection in the TT-Tree.

Similarly, the visit count $v_{i_{[j]}}$ is computed as:

$$\begin{aligned}
v_{i_{[j]}} &= \sum_{i_{j+1}=0}^{N_{j+1}} \cdots \sum_{i_d=0}^{N_d} \mathbf{V}_{(i_1, \dots, i_j, i_{j+1}, \dots, i_d)} \\
&\approx \sum_{i_{j+1}=0}^{N_{j+1}} \cdots \sum_{i_d=0}^{N_d} \mathbf{V}_{:,i_1,:}^1 \cdots \mathbf{V}_{:,i_j,:}^j \cdots \mathbf{V}_{:,i_d,:}^d.
\end{aligned} \tag{10}$$

Given $q_{i_{[j]}}$, $v_{i_{[j]}}$, and $v_{i_{[j-1]}}$, node expansion follows the UCB rule from (7). The TT-based representation enables parallel selection, which is typically non-trivial in node-based or table-based implementations. If no further expansion is possible, the current branch terminates. Otherwise, the branch is extended by one layer and followed by a simulation to the leaf. Rather than performing a random rollout, we leverage the TT model \mathbf{Q} as a global approximation of the decision tree to guide the simulation strategy via stochastic sampling, treating TT values as unnormalized probabilities. This enables parallel simulation and yields a top- k set of candidate solutions. After the simulation phase, optimal paths and their corresponding indices are identified, followed by backpropagation to update \mathbf{Q} and \mathbf{V} in preparation for the next iteration. During backpropagation, the visit count model \mathbf{V} is updated using a residual strategy. Since the newly visited indices are known, we adapt the standard TT-Cross algorithm into a guided version, where the residual tensor $\Delta \mathbf{V} \gamma^l$ is approximated using only one iteration over the specified index set $i_{[\gamma]}$ at layer γ . The value model \mathbf{Q} can also be updated in a similar manner to enhance approximation accuracy, but this

step can be omitted in practice to reduced runtime. In each iteration, a solution list \mathcal{S} is refreshed to maintain the top- k candidates. Our framework supports full parallelization across all MCTS components, unlike traditional MCTS methods, which typically allow only partial parallelization at the simulation stage (56). This significantly improves the convergence rate. Finally, the candidates obtained from TT-Tree Search are further refined using CMA-ES to correct for discretization errors in the continuous domain.

Theoretical proof

Since a decision tree can be equivalently represented as a tensor, we define a decision tree as *low-rank* if its corresponding tensor is low-rank. A tensor is considered low-rank if it can be well approximated using a decomposition format such as CP, Tucker, or TT (57), where the ranks are significantly smaller than the original tensor dimensions. For example, in the TT format, a tensor is low-rank if the TT ranks of the third-order cores satisfy $r_j \ll N_j$ for all j .

Here, we present three theoretical results to show that TTTS can efficiently converge to a bounded-error solution of the optimization problem defined in (1). First, we show that the bounded global optimum of a TT model can be retrieved efficiently with linear complexity. For decision trees that are low-rank, a TT model can be accurately constructed and yields a near-global solution due to its low approximation error. In the case of high-rank trees, TT approximation may incur larger errors. However, thanks to the exploration-exploitation mechanism of MCTS, the algorithm guarantees asymptotic convergence to the global optimum. Moreover, the TT representation enhances the search efficiency by guiding exploration and enabling parallel MCTS rollouts, significantly improving the convergence rate.

Theorem 1. *Given a TT model \mathcal{T} , the global optimum can be efficiently retrieved with linear time complexity.*

Proof. Given a TT representation, the value of any specific element can be accessed as:

$$\mathcal{T}(x_1, \dots, x_d) = \sum_{\gamma_1=1}^{r_1} \sum_{\gamma_2=1}^{r_2} \cdots \sum_{\gamma_{d-1}=1}^{r_{d-1}} \mathcal{T}^1(1, x_1, \gamma_1) \mathcal{T}^2(\gamma_1, x_2, \gamma_2) \cdots \mathcal{T}^d(\gamma_{d-1}, x_d, 1), \quad (11)$$

Algorithm 1 Tensor Train Tree Search (TTTS)

```

1: function TENSORTRAINTREESearch( $\mathbf{x}_0, \mathbf{z}, \tilde{\mathbf{Q}}, J, L, \Omega_w, \mathcal{I}$ )
2:   Input: Initial state  $\mathbf{x}_0$ , Condition var.  $\mathbf{z}$ , Augmented decision tree  $\tilde{\mathbf{Q}}$ , Objective function  $J$ ,
3:   Maximum iteration  $L$ , Domain  $\Omega_w = \{(w_1^{i_1}, \dots, w_d^{i_d}) : i_k \in \{1, \dots, N_k\}\}$ ,
4:   Index set  $\mathcal{I} \subseteq \{1, \dots, N_1\} \times \dots \times \{1, \dots, N_d\}$ 
5:   Hyperparameters: Number of solutions  $k$ , Exploration param.  $c$  # default:  $k = 10, c = 3$ 
6:   Output: Top- $k$  solution list  $\mathcal{S}$ 
7:   // ===== TT-Tree Initialization =====
8:    $\tilde{\mathbf{Q}} = \text{TT-Cross}(\tilde{\mathbf{Q}}), \mathbf{Q} \leftarrow \tilde{\mathbf{Q}}(\mathbf{z})$ 
9:   // ===== TT-Tree Search =====
10:   $i_0 \leftarrow \text{Node}(\mathbf{x}_0), \mathcal{V}_0 \leftarrow \mathbf{0}, \mathcal{S} = [ ]$ 
11:  for  $\ell = 1, 2, \dots, L$  do
12:    for  $j = 1, \dots, d$  do
13:       $q_{i_{[j]}} \leftarrow \text{Eq. (9)}, v_{i_{[j]}}, v_{i_{[j-1]}} \leftarrow \text{Eq. (10)}$ 
14:       $i_{[j]} \leftarrow \arg \max_{i_{[j]} \in \Omega_w}^k \left( \frac{q_{i_{[j]}}}{v_{i_{[j]}}} + c \cdot \sqrt{\frac{\log v_{i_{[j-1]}}}{v_{i_{[j]}}}} \right)$ 
15:      if  $i_j$  is not expanded then break
16:    end for
17:    for  $s = j + 1, \dots, d$  do
18:       $q_{i_{[s]}} \leftarrow \text{Eq. (9)}$ 
19:       $i_{[s]} \leftarrow \arg \max_{i_{[s]} \in \Omega}^{k_s} q_{i_{[s]}}$ 
20:    end for
21:     $\mathcal{W} \leftarrow \Omega_w(i_{[d]})$ 
22:     $i_{[d]}^* \leftarrow \arg \max_{i \in \mathcal{I}}^k J(\mathcal{W}_i)$ 
23:     $\mathbf{w}^* \leftarrow \arg \max_{\mathbf{w} \in \mathcal{W}}^k J(\mathbf{w})$ 
24:    for  $\gamma = 1, \dots, j$  do
25:       $\mathcal{V}_\gamma^l = \mathcal{V}_\gamma^{l-1} + \text{Guided-Cross}(\Delta \mathbf{V}_\gamma^l, i_{[\gamma]})$ 
26:    end for
27:     $\mathcal{S}_{aug} \leftarrow \text{append}(\mathcal{S}, \mathbf{w}^*)$ 
28:     $\mathcal{S} \leftarrow \arg \max_{\mathbf{w} \in \mathcal{S}_{aug}}^k J(\mathbf{w})$ 
29:  end for
30:  // ===== TT-Tree Refinement =====
31:   $\mathcal{S} \leftarrow \text{CMA-ES}(\mathcal{S})$ 
32:  return  $\mathcal{S}$ 
33: end function

```

where each \mathcal{T}^k is a TT core of size $r_{k-1} \times N_k \times r_k$, with N_k denoting the number of discretization points for x_k , and r_k representing the TT ranks, which are small for low-rank trees.

This shows that each element of \mathcal{T} can be expressed as a finite sum of products of separable TT cores. As a result, the global optimum of \mathcal{T} can be found through a dimension-wise optimization procedure that does not require convexity or differentiability. This process is analogous to traversing a fully evaluated tree: by selecting the node with the highest value at each layer, the optimal branch can be identified.

Specifically, we carry out this process in TT format. As illustrated in Fig. 8, a decision tree can be equivalently represented as a tensor, which can then be expressed in TT format for efficient computation. Based on (9), we compute the node values for each layer and choose the one with the highest value. By recursively traversing from the root to the final layer, the global optimum of the TT model is obtained, with a linear time complexity $\mathcal{O}(Ndr^2)$.

□

Theorem 2. *Consider a high-dimension tensor \mathbf{T} that is approximated by a low-rank TT model \mathcal{T} , with approximation error ϵ , the error of the found solution compared with the maximum value of \mathbf{T} is bounded with 2ϵ , namely*

$$\|\max \mathbf{T} - \mathbf{T}(\arg \max \mathcal{T})\| \leq 2\epsilon \quad (12)$$

Proof. Consider a discrete search space Ω , with $|\Omega| < \infty$. We aim to find

$$\mathbf{x}^* = \arg \max_{\mathbf{x} \in \Omega} \mathbf{T}(\mathbf{x}), \quad \mathbf{T}^* = \max_{\mathbf{x} \in \Omega} \mathbf{T}(\mathbf{x}).$$

Suppose we first approximate \mathbf{T} by a low-rank TT model \mathcal{T} , satisfying

$$\|\mathcal{T} - \mathbf{T}\|_{\infty} = \max_{\mathbf{x} \in \Omega} |\mathcal{T}(\mathbf{x}) - \mathbf{T}(\mathbf{x})| \leq \epsilon.$$

Then we can prove that

$$\begin{aligned} & \|\max \mathbf{T} - \mathbf{T}(\arg \max \mathcal{T})\| \\ & \leq \|\max \mathbf{T} - \max \mathcal{T}\| + \|\max \mathcal{T} - \mathbf{T}(\arg \max \mathcal{T})\| \\ & \leq 2\epsilon \end{aligned} \quad (13)$$

□

Theorem 3. *When the TT approximation error ϵ is non-negligible, TTTS retains the property of asymptotic global convergence, with TT representation significantly increasing the convergence speed.*

Proof. In a MCTS framework (with a finite-depth tree corresponding to the coordinates of $\mathbf{x} \in \Omega$), we initialize each leaf node x with $Q_0(\mathbf{x}) = \mathbf{Q}(\mathbf{x})$. A standard UCB-based selection rule then balances exploitation (nodes with high Q) and exploration (nodes that are under-visited).

Asymptotic Global Convergence. Because Ω is finite, a classical result states that if every node is explored infinitely often (i.e., the algorithm does not permanently abandon any branch), MCTS converges almost surely to the global maximum:

$$\lim_{l \rightarrow \infty} \max_{\mathbf{x} \in \Omega} |\widehat{Q}_l(\mathbf{x}) - \mathbf{T}(\mathbf{x})| = 0,$$

hence $\arg \max_{\mathbf{x}} \widehat{Q}_l(\mathbf{x}) \rightarrow \arg \max_{\mathbf{x}} \mathbf{T}(\mathbf{x})$, where \widehat{Q}_l is the node value estimate after l iterations.

TT Prior for Faster Convergence. A good TT approximation further *accelerates* convergence in practice. If \mathcal{T} is close to \mathbf{T} in $\|\cdot\|_\infty$ -norm, the initial value assignments guide MCTS away from evidently suboptimal nodes. Indeed, let $\mathbf{x}^* = \arg \max \mathcal{T}(\mathbf{x})$. Then

$$|\mathcal{T}(\mathbf{x}^*) - \mathbf{T}(\mathbf{x}^*)| \leq \epsilon.$$

Any node \mathbf{y} with $\mathcal{T}(\mathbf{y}) \leq \mathcal{T}^* - 2\epsilon$ satisfies $\mathbf{T}(\mathbf{y}) \leq \mathcal{T}(\mathbf{y}) + \epsilon \leq \mathcal{T}^* - \epsilon \leq \mathbf{T}(\mathbf{x}^*)$, so \mathbf{y} cannot exceed \mathbf{x}^* in true value. Hence, the UCB mechanism quickly allocates fewer visits to such nodes, reducing wasted exploration and sharpening the focus on genuinely near-optimal candidates. Mathematically, this effect appears in “gap-based” analyses for bandit algorithms, where an accurate prior \mathcal{T} increases the effective gap of suboptimal nodes, thus lowering their exploration burden. Consequently, while MCTS still guarantees asymptotic global convergence, an accurate TT approximation substantially speeds up the reaching of near-optimal solutions in finite time.

□

References and Notes

1. A. Goldenberg, B. Benhabib, R. Fenton, A complete generalized solution to the inverse kinematics of robots. *IEEE Journal on Robotics and Automation* **1** (1), 14–20 (2003).
2. T. Marcucci, M. Petersen, D. von Wrangel, R. Tedrake, Motion planning around obstacles with convex optimization. *Science robotics* **8** (84), eadf7843 (2023).
3. M. Toussaint, Logic-geometric programming: an optimization-based approach to combined task and motion planning, in *Proceedings of the 24th International Conference on Artificial Intelligence* (2015), pp. 1930–1936.
4. M. T. Mason, Mechanics and planning of manipulator pushing operations. *International Journal of Robotics Research (IJRR)* **5** (3), 53–71 (1986).
5. M. T. Mason, Progress in nonprehensile manipulation. *International Journal of Robotics Research (IJRR)* **18** (11), 1129–1141 (1999).
6. T. S. Lembono, A. Paolillo, E. Pignat, S. Calinon, Memory of motion for warm-starting trajectory optimization. *IEEE Robotics and Automation Letters (RA-L)* **5** (2), 2594–2601 (2020).
7. T. Xue, H. Girgin, T. S. Lembono, S. Calinon, Demonstration-guided optimal control for long-term non-prehensile planar manipulation, in *Proc. IEEE Intl Conf. on Robotics and Automation (ICRA)* (2023), pp. 4999–5005.
8. S. M. LaValle, *Planning algorithms* (Cambridge university press) (2006).
9. L. E. Kavraki, P. Svestka, J.-C. Latombe, M. H. Overmars, Probabilistic roadmaps for path planning in high-dimensional configuration spaces. *IEEE transactions on Robotics and Automation* **12** (4), 566–580 (1996).
10. P. E. Hart, N. J. Nilsson, B. Raphael, A formal basis for the heuristic determination of minimum cost paths. *IEEE transactions on Systems Science and Cybernetics* **4** (2), 100–107 (1968).
11. Z. Wang, M. J. Grant, Constrained trajectory optimization for planetary entry via sequential convex programming. *Journal of Guidance, Control, and Dynamics* **40** (10), 2603–2615 (2017).

12. D. Malyuta, *et al.*, Convex optimization for trajectory generation: A tutorial on generating dynamically feasible trajectories reliably and efficiently. *IEEE Control Systems Magazine* **42** (5), 40–113 (2022).
13. Y. Lin, S. Saripalli, Sampling-based path planning for UAV collision avoidance. *IEEE Transactions on Intelligent Transportation Systems* **18** (11), 3179–3192 (2017).
14. T. Pang, H. T. Suh, L. Yang, R. Tedrake, Global planning for contact-rich manipulation via local smoothing of quasi-dynamic contact models. *IEEE Transactions on Robotics* (2023).
15. M. Posa, C. Cantu, R. Tedrake, A direct method for trajectory optimization of rigid bodies through contact. *International Journal of Robotics Research (IJRR)* **33** (1), 69–81 (2014).
16. J. Moura, T. Stouraitis, S. Vijayakumar, Non-prehensile planar manipulation via trajectory optimization with complementarity constraints, in *Proc. IEEE Intl Conf. on Robotics and Automation (ICRA)* (2022), pp. 970–976.
17. R. Natarajan, H. Choset, M. Likhachev, Interleaving graph search and trajectory optimization for aggressive quadrotor flight. *IEEE Robotics and Automation Letters* **6** (3), 5357–5364 (2021).
18. M. Mukadam, J. Dong, X. Yan, F. Dellaert, B. Boots, Continuous-time Gaussian process motion planning via probabilistic inference. *International Journal of Robotics Research (IJRR)* **37** (11), 1319–1340 (2018).
19. T. Xue, A. Razmjoo, S. Calinon, D-LGP: Dynamic Logic-Geometric Program for Reactive Task and Motion Planning, in *Proc. IEEE Intl Conf. on Robotics and Automation (ICRA)* (2024), pp. 14888–14894.
20. C. R. Garrett, *et al.*, Integrated task and motion planning. *Annual review of control, robotics, and autonomous systems* **4** (1), 265–293 (2021).
21. J. F. Magee, *Decision trees for decision making* (Harvard Business Review Brighton, MA, USA) (1964).
22. B. Rivière, J. Lathrop, S.-J. Chung, Monte Carlo tree search with spectral expansion for planning with dynamical systems. *Science Robotics* **9** (97), eado1010 (2024).

23. Z. Li, Q. Chen, V. Koltun, Combinatorial optimization with graph convolutional networks and guided tree search. *Advances in neural information processing systems* **31** (2018).
24. D. Silver, *et al.*, Mastering the game of Go with deep neural networks and tree search. *nature* **529** (7587), 484–489 (2016).
25. S. Shetty, T. Lembono, T. Löw, S. Calinon, Tensor Train for Global Optimization Problems in Robotics. *International Journal of Robotics Research (IJRR)* **43** (6), 811–839 (2024), doi: 10.1177/02783649231217527.
26. K. Sozykin, *et al.*, TTOpt: A maximum volume quantized tensor train-based optimization and its application to reinforcement learning. *Advances in neural information processing systems* **35**, 26052–26065 (2022).
27. I. Oseledets, E. Tyrtyshnikov, TT-cross approximation for multidimensional arrays. *Linear Algebra and its Applications* **432** (1), 70–88 (2010).
28. D. V. Savostyanov, I. V. Oseledets, Fast adaptive interpolation of multi-dimensional arrays in tensor train format. *The 2011 International Workshop on Multidimensional (nD) Systems* pp. 1–8 (2011).
29. R. Holladay, T. Lozano-Pérez, A. Rodriguez, Robust planning for multi-stage forceful manipulation. *International Journal of Robotics Research (IJRR)* **43** (3), 330–353 (2024).
30. T. Xue, A. Razmjoo, S. Shetty, S. Calinon, Logic-Skill Programming: An Optimization-based Approach to Sequential Skill Planning, in *Proc. Robotics: Science and Systems (RSS)* (2024).
31. N. Doshi, F. R. Hogan, A. Rodriguez, Hybrid differential dynamic programming for planar manipulation primitives, in *Proc. IEEE Intl Conf. on Robotics and Automation (ICRA)* (2020), pp. 6759–6765.
32. T. Xue, A. Razmjoo, S. Shetty, S. Calinon, Robust Manipulation Primitive Learning via Domain Contraction, in *Proc. Conference on Robot Learning (CoRL)* (2024).
33. T. Xue, A. Razmjoo, S. Shetty, S. Calinon, Robust Contact-rich Manipulation through Implicit Motor Adaptation. *International Journal of Robotics Research (IJRR)* (2025).

34. E. Todorov, T. Erez, Y. Tassa, Mujoco: A physics engine for model-based control, in *2012 IEEE/RSJ international conference on intelligent robots and systems* (IEEE) (2012), pp. 5026–5033.
35. J. Liang, *et al.*, Gpu-accelerated robotic simulation for distributed reinforcement learning, in *Conference on Robot Learning* (PMLR) (2018), pp. 270–282.
36. G. Authors, Genesis: A Universal and Generative Physics Engine for Robotics and Beyond (2024).
37. D. Mayne, A second-order gradient method for determining optimal trajectories of non-linear discrete-time systems. *International Journal of Control* **3** (1), 85–95 (1966).
38. Y. Tassa, T. Erez, E. Todorov, Synthesis and stabilization of complex behaviors through online trajectory optimization, in *2012 IEEE/RSJ International Conference on Intelligent Robots and Systems* (IEEE) (2012), pp. 4906–4913.
39. W. Li, E. Todorov, Iterative linear quadratic regulator design for nonlinear biological movement systems, in *International Conference on Informatics in Control, Automation and Robotics* (SciTePress), vol. 2 (2004), pp. 222–229.
40. N. Ratliff, M. Zucker, J. A. Bagnell, S. Srinivasa, CHOMP: Gradient optimization techniques for efficient motion planning, in *Proc. IEEE Intl Conf. on Robotics and Automation (ICRA)* (2009), pp. 489–494.
41. J. Schulman, *et al.*, Motion planning with sequential convex optimization and convex collision checking. *International Journal of Robotics Research (IJRR)* **33** (9), 1251–1270 (2014).
42. S. Karaman, E. Frazzoli, Sampling-based algorithms for optimal motion planning. *International Journal of Robotics Research (IJRR)* **30** (7), 846–894 (2011).
43. J. D. Gammell, S. S. Srinivasa, T. D. Barfoot, Batch informed trees (BIT*): Sampling-based optimal planning via the heuristically guided search of implicit random geometric graphs, in *Proc. IEEE Intl Conf. on Robotics and Automation (ICRA)* (2015), pp. 3067–3074.

44. N. Hansen, S. D. Müller, P. Koumoutsakos, Reducing the time complexity of the derandomized evolution strategy with covariance matrix adaptation (CMA-ES). *Evolutionary computation* **11** (1), 1–18 (2003).
45. O. Salzman, D. Halperin, Asymptotically near-optimal RRT for fast, high-quality motion planning. *IEEE Transactions on Robotics* **32** (3), 473–483 (2016).
46. R. Coulom, Efficient selectivity and backup operators in Monte-Carlo tree search, in *International conference on computers and games* (Springer) (2006), pp. 72–83.
47. C. B. Browne, *et al.*, A survey of monte carlo tree search methods. *IEEE Transactions on Computational Intelligence and AI in games* **4** (1), 1–43 (2012).
48. D. Silver, *et al.*, Mastering the game of go without human knowledge. *nature* **550** (7676), 354–359 (2017).
49. H. Choset, K. M. Lynch, S. Hutchinson, G. A. Kantor, W. Burgard, *Principles of robot motion: theory, algorithms, and implementations* (MIT press) (2005).
50. R. Deits, R. Tedrake, Computing large convex regions of obstacle-free space through semidefinite programming, in *Workshop on the Algorithmic Foundations of Robotics (WAFR)* (Springer) (2015), pp. 109–124.
51. T. Marcucci, J. Umenberger, P. Parrilo, R. Tedrake, Shortest paths in graphs of convex sets. *SIAM Journal on Optimization* **34** (1), 507–532 (2024).
52. T. Anthony, Z. Tian, D. Barber, Thinking fast and slow with deep learning and tree search. *Advances in neural information processing systems* **30** (2017).
53. B. Kim, K. Lee, S. Lim, L. Kaelbling, T. Lozano-Pérez, Monte carlo tree search in continuous spaces using voronoi optimistic optimization with regret bounds, in *Proceedings of the AAAI Conference on Artificial Intelligence*, vol. 34 (2020), pp. 9916–9924.
54. L. Liberti, Undecidability and hardness in mixed-integer nonlinear programming. *RAIRO-Operations Research* **53** (1), 81–109 (2019).

55. A. Cichocki, *et al.*, Tensor networks for dimensionality reduction and large-scale optimization: Part 1 low-rank tensor decompositions. *Foundations and Trends® in Machine Learning* **9** (4-5), 249–429 (2016).
56. G. M. B. Chaslot, M. H. Winands, H. J. van Den Herik, Parallel monte-carlo tree search, in *Computers and Games: 6th International Conference, CG 2008, Beijing, China, September 29-October 1, 2008. Proceedings 6* (Springer) (2008), pp. 60–71.
57. L. Grasedyck, D. Kressner, C. Tobler, A literature survey of low-rank tensor approximation techniques. *GAMM-Mitteilungen* **36** (1), 53–78 (2013).
58. I. V. Oseledets, Tensor-train decomposition. *SIAM Journal on Scientific Computing* **33** (5), 2295–2317 (2011).

Acknowledgments

Funding: This work was supported by the China Scholarship Council (grant No.202106230104), and by the State Secretariat for Education, Research and Innovation in Switzerland for participation in the European Commission’s Horizon Europe Program through the INTELLIMAN project (<https://intelliman-project.eu/>, HORIZON-CL4-Digital-Emerging Grant 101070136) and the SESTOSENSO project (<http://sestosenso.eu/>, HORIZON-CL4-Digital-Emerging Grant 101070310).

Author contributions: The algorithm conceptualization, theoretical development, software implementation, and experimental design were conducted by T.X., under the guidance and critical review of S.C. The Genesis environment setup and robot visualizations were implemented by Y.Z. The real-robot bimanual manipulation experiments were primarily carried out by A.R. S.C. supervised the research. All authors reviewed the manuscript.

Competing interests: There are no competing interests to declare.

Data and materials availability: All data and code used to generate the results in this paper will be made available at our project webpage (<https://sites.google.com/view/tt-ts>) upon acceptance.

Supplementary materials

Supplementary Text

Table S1

Movie S1

Supplementary Materials for

Unifying Robot Optimization: Monte Carlo Tree Search with

Tensor Factorization

Teng Xue^{1,2*}, Amirreza Razmjoo^{1,2†}, Yan Zhang^{1,2†}, Sylvain Calinon^{1,2}

¹Idiap Research Institute, Martigny & 1920, Switzerland

²École Polytechnique Fédérale de Lausanne(EPFL), Lausanne & 1015, Switzerland

*Corresponding author. Email: teng.xue@idiap.ch

†These authors contributed equally to this work. The authors' names are listed in alphabetical order.

This PDF file includes:

Supplementary Text

Table S1

Caption for Movie S1

Other Supplementary Materials for this manuscript:

Movie S1

Project Webpage: <https://sites.google.com/view/tt-ts>

Materials and Methods

Discrete Tensor Approximation of Functions

A multivariate function $F(x_1, \dots, x_d)$ defined over a Cartesian domain $I_1 \times \dots \times I_d$ can be discretized into a tensor \mathcal{F} by evaluating it at a grid of points. Specifically, each tensor element is defined as $\mathcal{F}_{i_1, \dots, i_d} = F(x_1^{i_1}, \dots, x_d^{i_d})$, with indices $i_k \in 1, \dots, n_k$. Values of the original continuous function can then be approximated via interpolation of the tensor elements.

Tensor Train (TT) Decomposition

Direct storage and computation of high-dimensional tensors ($O(n^d)$ complexity) is impractical. Similar to matrix factorization techniques, Tensor Networks address this issue by factorizing the tensor into compact representations. The Tensor Train (TT) decomposition is a specific type of Tensor Networks that represents a d -dimensional tensor as a sequence of low-rank, three-dimensional tensors called *cores*. A tensor element in TT format is computed as:

$$\mathcal{F}(i_1, \dots, i_d) = \mathcal{F}_{:,i_1,:}^1 \mathcal{F}_{:,i_2,:}^2 \cdots \mathcal{F}_{:,i_d,:}^d, \quad (\text{S1})$$

where $\mathcal{F}_{:,i_k,:}^k \in \mathbb{R}^{r_{k-1} \times r_k}$ denotes the i_k -th slice of the k -th core. TT decompositions are guaranteed to exist and can significantly reduce complexity. Algorithms such as TT-SVD (58) and TT-Cross (27, 28) facilitate efficient computation and storage. Specifically, TT-Cross enables tensor construction without fully evaluating or storing all tensor elements, making it suitable for approximating high-dimensional tensors.

Continuous Function Approximation via TT

The discretized TT representation can approximate continuous functions by interpolating across tensor cores. For instance, using linear interpolation between core slices, each core defines a matrix-valued interpolation:

$$\mathbf{F}^k(x_k) = \frac{x_k - x_k^{i_k}}{x_k^{i_{k+1}} - x_k^{i_k}} \mathcal{F}_{:,i_{k+1},:}^k + \frac{x_k^{i_{k+1}} - x_k}{x_k^{i_{k+1}} - x_k^{i_k}} \mathcal{F}_{:,i_k,:}^k, \quad (\text{S2})$$

with $x_k^{i_k} \leq x_k \leq x_k^{i_{k+1}}$. The resulting continuous approximation becomes:

$$F(x_1, \dots, x_d) \approx \mathbf{F}^1(x_1) \cdots \mathbf{F}^d(x_d), \quad (\text{S3})$$

allowing representation and approximation of functions with mixed discrete-continuous domains efficiently.

Global Optimization using Tensor Train (TTGO)

In global optimization, the objective is to find decision variables \mathbf{x} that maximize a given function $f(\mathbf{x})$. The TTGO framework (25) approaches this problem by interpreting $f(\mathbf{x})$ as an unnormalized density function $F(\mathbf{x})$ through a suitable transformation that preserves the ordering of optima. This function $F(\mathbf{x})$ is then approximated in the Tensor Train (TT) format via the TT-Cross algorithm, yielding a structured and compact representation:

$$F(x_1, \dots, x_d) \approx \sum_{\gamma_1=1}^{r_1} \sum_{\gamma_2=1}^{r_2} \cdots \sum_{\gamma_{d-1}=1}^{r_{d-1}} \mathcal{F}^1(1, x_1, \gamma_1) \mathcal{F}^2(\gamma_1, x_2, \gamma_2) \cdots \mathcal{F}^d(\gamma_{d-1}, x_d, 1), \quad (\text{S4})$$

where each TT core \mathcal{F}^k is a tensor of size $r_{k-1} \times N_k \times r_k$, with N_k denoting the discretization resolution of the k -th variable and r_k representing the TT ranks.

The resulting TT model provides a low-rank approximation that supports efficient optimization. Instead of relying on exhaustive grid search, which scales poorly with dimensionality ($\mathcal{O}(N^d)$), TTGO exploits the tensor structure to perform efficient dimension-wise search. This leads to a computational complexity of $\mathcal{O}(Ndr^2)$, where N is the typical number of discretization points per dimension and r is the maximum TT rank.

Importantly, TTGO requires no gradient information, making it highly applicable to black-box or non-differentiable functions. Its effectiveness has been demonstrated in high-dimensional and non-convex scenarios. For more detailed algorithmic discussions, we refer readers to foundational works in TT methods (58, 26).

Experiments

Experimental hyperparameter

In our experiments, we utilized an NVIDIA GeForce RTX 3090 GPU with 24 GB of memory. The tolerance for the TT-Cross approximation was set to $\epsilon = 10^{-3}$. Table S1 summarizes the

Table S1: Hyperparameters employed for different tasks.

Task	Batch Size	Num. MCTS	Num. Discret.	Num. Sim.	r_{max}	Pop. Size	CMA-ES Iter.
3-joint IK	1000	5	20	1000	21	25	20
7-joint IK	500	5	20	1000	21	25	20
3-joint MP	1000	5	20	1000	41	25	20
7-joint MP	500	5	20	1000	21	25	20
Multi-stage MP	1000	5	50	1000	41	25	20
Whole-body Manipulation	500	1	20	10	21	25	20

hyperparameters applied across different tasks. *Batch size* indicates the maximum number of parallel environments; *Num. MCTS* denotes the number of independent MCTS instances executed concurrently; and *Num. Sim.* specifies the number of parallel environments used during the simulation phase. *Num. Discret.* refers to the discretization granularity of the state and action spaces. The parameter r_{max} defines the maximum TT rank employed during TT-Tree initialization via TT-Cross. *Pop. Size* and *CMA-ES Iter.* are the population size and iteration count used in the CMA-ES refinement step, respectively.

Cost Function

Cost function for inverse kinematics. In the inverse kinematics (IK) setting, the goal is to find a joint configuration $\mathbf{q} \in \mathbb{R}^n$ such that the robot’s end-effector reaches a desired target position while avoiding collisions and maintaining reasonable deviation from the current posture. The total cost function used is defined as:

$$d_{total} = 50 d_{goal} + d_{obst}.$$

The term d_{goal} penalizes the distance between the forward kinematics output of the proposed joint configuration and the desired end-effector position:

$$d_{goal} = \|\mathbf{eef}_{pos}(\mathbf{q}) - \mathbf{x}_{goal}\|_2.$$

Here, \mathbf{x}_{goal} is the target pose of the end-effector, and $\mathbf{eef}_{pos}(\mathbf{q})$ denotes the pose of the end-effector computed using forward kinematics at joint configuration \mathbf{q} .

The term d_{obst} penalizes collisions by summing binary collision indicators for the final robot

configuration:

$$d_{\text{obst}} = \sum_{i=1}^{N_{\text{links}}} \text{collides}_i(\mathbf{q}),$$

where $\text{collides}_i(\mathbf{q}) \in \{0, 1\}$ indicates whether the i -th link is in collision.

Cost function for motion planning. The total cost function used for trajectory optimization is composed of three terms: a goal-reaching cost, a collision avoidance cost, and a control smoothness cost. The overall cost is defined as:

$$d_{\text{total}} = 50 d_{\text{goal}} + d_{\text{obst}} + 0.1 d_{\text{control}}.$$

The first term, d_{goal} , encourages the robot to reach the desired target position. It is computed as the Euclidean distance between the current end-effector position and the goal:

$$d_{\text{goal}} = \|\text{eef}_{\text{pos}} - \mathbf{x}_{\text{goal}}\|_2,$$

where eef_{pos} denotes the Cartesian position of the robot's end-effector at the final time step, and \mathbf{x}_{goal} is the desired target position.

The second term, d_{obst} , penalizes trajectories that result in collisions. It is computed by summing binary collision indicators over the trajectory:

$$d_{\text{obst}} = \sum_{t=1}^T \text{collisions}_t,$$

where $\text{collisions}_t \in \{0, 1\}$ is a binary variable indicating whether a collision occurs at time step t .

The third term, d_{control} , measures the smoothness of the joint trajectory. It compares the total length of the path in joint space with the direct distance between the start and end configurations:

$$d_{\text{control}} = \frac{\sum_{t=1}^T \|\mathbf{q}_t - \mathbf{q}_{t-1}\|_2}{\|\mathbf{q}_T - \mathbf{q}_0\|_2 + \varepsilon}.$$

Here, \mathbf{q}_t represents the robot's joint configuration at time step t , and ε is a small positive constant added for numerical stability. We set $\varepsilon = 10^{-6}$ in our experiments.

Cost function for multi-stage motion planning. In the planar pushing setting, the objective is to compute a sequence of discrete contact modes and continuous robot velocities that move an object

from its initial state to a target pose. The total cost combines two components: a state reaching cost and a control effort cost. It is defined as:

$$d_{\text{total}} = d_{\text{state}} + 0.01 d_{\text{action}}.$$

The state cost d_{state} evaluates how far the final state $\mathbf{x}_T \in \mathbb{R}^3$ (position and orientation of the object) is from the target pose $\mathbf{x}_{\text{target}} \in \mathbb{R}^3$. It is defined as:

$$d_{\text{state}} = \left\| \mathbf{x}_T^{\text{pos}} - \mathbf{x}_{\text{target}}^{\text{pos}} \right\|_2 + 0.1 \left| \theta_T - \theta_{\text{target}} \right|,$$

where:

- $\mathbf{x}_T^{\text{pos}} = [x_{1T}, x_{2T}]^\top$ is the object's final position
- θ_T is the final orientation
- $\mathbf{x}_{\text{target}}^{\text{pos}}$ and θ_{target} are the desired position and orientation

The action cost d_{action} penalizes the total effort of the pushing trajectory, where each control input $\mathbf{u}_t \in \mathbb{R}^2$ represents a planar velocity vector. The total control cost is the sum of the norms of all pushing actions:

$$d_{\text{action}} = \sum_{k=1}^K \sum_{t=1}^T \|\mathbf{u}_t\|_2.$$

These actions are generated based on a discrete contact face selection and continuous parameters defining a trajectory. The discrete mode $i_t \in \{1, 2, 3, 4\}$ specifies which face of the object is being pushed at each time.

The final cost balances reaching the target pose accurately with minimizing the pushing effort, with a small weight on the latter to avoid excessive motion without overconstraining the optimization.

Cost function for whole-body manipulation. In the bimanual whole-body manipulation setting, the objective is to control two arms collaboratively to manipulate an object (e.g., a box) toward

a target pose while maintaining effective contact and avoiding awkward configurations. The total cost function is composed of five terms:

$$d_{\text{total}} = d_{\text{pos}} + 50 d_{\text{orn}} + 0.1 d_{\text{control}} - d_{\text{contact}} + 5 \delta_{\text{eef}},$$

where d_{pos} penalizes deviation of the box's final position from the target:

$$d_{\text{pos}} = \|\mathbf{p}_T^{\text{box}} - \mathbf{p}_{\text{target}}\|_2.$$

$\mathbf{p}_T^{\text{box}} \in \mathbb{R}^3$ is the final box position and $\mathbf{p}_{\text{target}}$ is the desired position. d_{orn} measures orientation alignment between the final box orientation and the target orientation, namely

$$d_{\text{orn}} = |\theta_T^{\text{box}} - \theta_{\text{target}}|.$$

d_{control} is a regularization term that penalizes excessive joint movement across the trajectory:

$$d_{\text{control}} = \sum_{t=0}^T \|\mathbf{q}_{t+1} - \mathbf{q}_t\|_2,$$

where $\mathbf{q}_t \in \mathbb{R}^n$ is the full-body joint configuration at time step t .

d_{contact} rewards the maintenance of valid bimanual contact. Let $c_t^L, c_t^R \in \{0, 1\}$ be binary contact flags for the left and right hands. Then:

$$d_{\text{contact}} = \sum_{t=1}^T \mathbb{I}[c_t^L = 1 \wedge c_t^R = 1],$$

where $\mathbb{I}[\cdot]$ is the indicator function. This term is subtracted from the total cost to encourage simultaneous dual-arm contact.

δ_{eef} is a binary term that penalizes configurations where the two arms are too close to each other, in order to avoid self-collision:

$$\delta_{\text{eef}} = \mathbb{I}[\|\mathbf{x}^{\text{eef}_0} - \mathbf{x}^{\text{eef}_1}\|_2 < 0.3],$$

where $\mathbf{x}^{\text{eef}_i}$ is the Cartesian position of the i -th end-effector.

The cost function encourages accurate placement and orientation of the manipulated object, smooth and efficient joint trajectories, persistent bimanual contact, and physically feasible arm configurations.

Caption for Movie S1. Diverse robotic tasks solved by TTTS. We applied our approach to a diverse set of robotic tasks, including inverse kinematics, motion planning, multi-stage motion planning, and bimanual whole-body manipulation. This video showcases the results achieved using TTTS, including visualizations, simulated trajectories, and real-world experiments. It serves as a supplement to the results presented in Fig. 1 and Fig. 7.